

Single-bonded allotrope of nitrogen predicted at high pressure**HPSTAR
489-2017**

Adebayo A. Adeleke,¹ Michael J. Greschner,¹ Arnab Majumdar,¹ Biao Wan,² Hanyu Liu,³
Zhiping Li,⁴ Huiyang Gou,^{2,4,*} and Yansun Yao^{1,5,†}

¹*Department of Physics and Engineering Physics, University of Saskatchewan, Saskatoon, Saskatchewan S7N 5E2, Canada*

²*Center for High Pressure Science and Technology Advanced Research, Beijing 100094, China*

³*Geophysical Laboratory, Carnegie Institution of Washington, 5251 Broad Branch Road NW, Washington, DC 20015, USA*

⁴*Key Laboratory of Applied Chemistry, College of Environmental and Chemical Engineering,
Yanshan University, Qinhuangdao 066004, China*

⁵*Canadian Light Source, Saskatoon, Saskatchewan S7N 2V3, Canada*

(Received 21 December 2016; published 26 December 2017)

An allotrope of nitrogen formed solely by N-N single bonds is predicted to exist between 100 and 150 GPa. The crystal structure has the *Pccn* symmetry and is characterized by a distorted tetrahedral network consisting of fused N₈, N₁₀, and N₁₂ rings. Stability of this structure is established by phonon and vibrational free energy calculations at 0 K and finite temperatures. The simulated x-ray diffraction pattern of the *Pccn* phase is compared to the pattern of a recently synthesized nitrogen phase at the same *P-T* conditions, which suggests that the *Pccn* phase is likely a minor component of the latter. The *Pccn* phase is expected to form above the stability field of the cubic gauche (cg) phase. The outstanding metastability of this phase is attributed to the intrinsic stability of the *sp*³ bonding as well as the energetically favorable dihedral angles between N-N single bonds, in either *gauche* or *trans* conformation. The prediction of another single-bonded phase of nitrogen after the lab-synthesized cg phase will stimulate research on metastable phases of nitrogen and their applications as high-energy-density materials.

DOI: 10.1103/PhysRevB.96.224104

I. INTRODUCTION

Elemental nitrogen has been extensively investigated as a possible high-energy-density material (HEDM) under extreme conditions. At low pressures and temperatures, nitrogen forms chemically inert van der Waals solids consisting of triple-bonded N₂ molecules. At extremely high pressures and temperatures, nitrogen can transform to single-bonded extended structures. Due to a large amount of energy stored in the single bonds, the latter are efficient energy carriers, both in pure forms and compounds [1–4]. Allotropes formed solely by N-N single bonds could potentially be used as HEDMs, which are not only energy efficient but also environmentally friendly, producing only nontoxic N₂ during energy release. The single-bonded nitrogen was initially perceived to have the same crystal structures as isovalent black phosphorus (BP) or α -arsenic (A7), but in 1992, Mailhiot *et al.* predicted a unique structure composed of fused N₁₀ rings connected in a way that all dihedral angles between N-N single bonds are in energetically favorable gauche helicity [5]. This “cubic gauche” (cg) structure was later confirmed to be a thermodynamic ground state of nitrogen at high pressures. In the last two decades, new structures of nitrogen have been extensively searched for using various theoretical methods, which unearthed many interesting structures consisting of zero-, one-, two-, and three-dimensional motifs, including larger molecules (0D) [6,7], chains (1D) [8,9], chaired webs (1D-2D) [10], layers (2D) [11], layered boats (2D-3D), and cages (3D) [12]. A theoretical high-pressure zero-temperature phase transition sequence appears to be acceptable today, that is, from the molecular phase \rightarrow cg \rightarrow layered structure \rightarrow

cagelike structure in the gigapascal pressure region, and to a metallic salt structure at terapascal pressures [13–15].

Experimentally, a great amount of effort has been devoted to the synthesis of single-bonded nitrogen under extreme conditions. Early evidence of nonmolecular nitrogen at high pressure was reported by several groups, while the realized structures were likely amorphous [16–18]. In 2004, the first crystalline form, the long-sought cg phase, at high pressure (>120 GPa) and high temperatures (>2500 K) was successfully synthesized by Eremets *et al.* [3]. Later, the cg phase was synthesized again at different pressure-temperature conditions [19–21]. In 2014, another crystalline phase was synthesized above 120 GPa by Tomasino *et al.* [4] which was believed to have a single-bonded structure as well. However, this phase was found to mix with other phases (likely, amorphous and cg), making the structure identification challenging. The difficulties preclude a full-pattern Rietveld refinement of the experimental x-ray diffraction (XRD) data, but the Le Bail profiling suggests the structure is similar to a *Pba2* structure predicted by Ma *et al.* [14]. The exact structure of this phase is yet to be identified, which motivates the present study.

In this study, we investigate the structures of the recently synthesized phase by Tomasino *et al.* through the application of the first-principles metadynamics method. The *Pba2* structure is found to be consistent with, but not sufficient to reproduce, the reported XRD pattern. We propose an orthorhombic structure with the *Pccn* space group, which is energetically competitive with the *Pba2* structure in the same *P-T* region of the synthesis. The simulated XRD pattern for the 1:2 mixture of the *Pccn* and *Pba2* structures matches very well the experimental data. In particular, several low angle 2θ peaks in the experimental XRD pattern are systematic absences in the *Pba2* structure but can be satisfactorily explained by the *Pccn* structure. The *Pccn* structure is entirely single-bonded consisting of fused N₈, N₁₀, and N₁₂ rings, as opposed to

*Corresponding author: huiyang.gou@gmail.com

†Corresponding author: yansun.yao@usask.ca

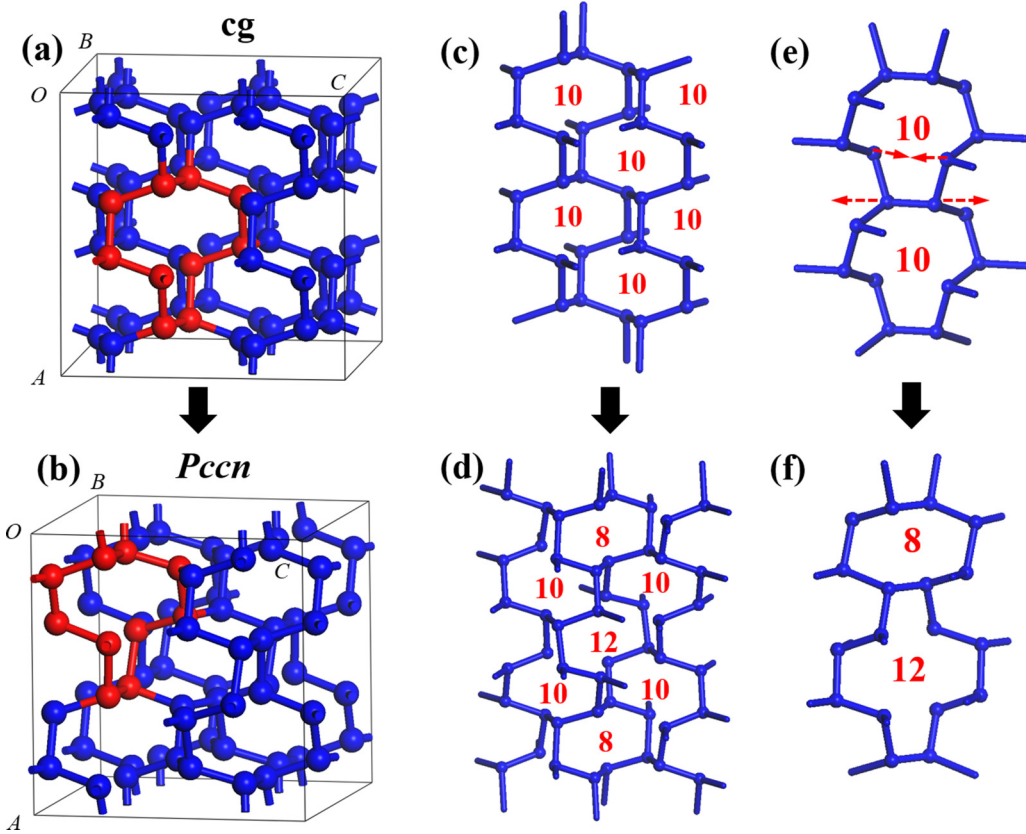


FIG. 1. (a) and (b) The *cg* and *Pccn* structures. A N_8 ring is highlighted in red (shade) in each structure. (c) Construction of the *cg* structure by fused N_{10} rings. (d) Construction of the *Pccn* structure by fused N_8 , N_{10} , and N_{12} rings. (e) and (f) Transition mechanism between an array of fused N_{10} rings to an array of alternating N_8 and N_{12} rings. Arrows in (e) indicate the bond-breaking/forming directions.

the *Pba2* structure which has fused N_7 rings. The *Pccn* structure was found to be dynamically stable in the *P-T* region of the synthesis by phonon and vibrational free energy calculations.

II. COMPUTATIONAL DETAILS

New structure formation under high-temperature, high-pressure conditions was simulated using the metadynamics method [22,23] combined with the projector-augmented plane wave (PAW) method [24] as implemented in the Vienna *ab initio* Simulation Package (VASP) [25]. A 5-electron tight PAW potential with the Perdew-Burke-Ernzerhof (PBE) functional [26] was used with a 900 eV kinetic energy cutoff. Various simulation cells consisting of 32 to 96 nitrogen atoms were employed along with a k spacing of $2\pi \times 0.08 \text{ \AA}^{-1}$ for Brillouin zone (BZ) sampling. A metadynamics simulation was carried out in the pressure range of 100–300 GPa and in the temperature range of 1000–2500 K. The driving force that guides the evolution of the structure is the derivative of the enthalpy (H) with respect to the simulation cell matrix. In the present study, the scaled components of the edge vectors of the simulation supercell were used as collective variables [22]. The Gaussian width (W) and height (δs), related by $W \approx \delta s^2$, were chosen to be 225 kbar \AA^3 and 15 (kbar \AA^3) $^{1/2}$, respectively. A step length of 0.03 was employed for h -space sampling. The potential energy surface of nitrogen was

searched for up to 500 metasteps, where each metastep consists of a first-principles molecular dynamics (MD) simulation employing an *NVT* ensemble for 0.4 ps. A finer k spacing of $2\pi \times 0.03 \text{ \AA}^{-1}$ was used in structural optimization and enthalpy calculations. First-principles MD simulations were performed at high temperatures for candidate structures using the VASP program, employing an isothermal-isobaric (*NPT*) ensemble with Langevin dynamics. The anharmonic vibrational density of states (vDOS) was obtained from the 20 ps MD trajectory (sampled with a 2 fs time interval) after 3 ps equilibrium time. Possible structures at pressures of 100–300 GPa were also searched for using the CALYPSO code [27,28] and random searching method [29] within a 64 atoms/unit cell limit. Harmonic phonon calculations were performed using the linear response Hessian matrix obtained using the VASP program and postprocessed using the PHONOPY code [30]. The obtained phonon results were cross-checked using the QUANTUM ESPRESSO package [31] with norm-conserving pseudopotentials and an energy cutoff of 80 Ry, along with a $6 \times 6 \times 6$ q -point mesh and a $12 \times 12 \times 12$ k -point mesh. The crystal-orbital Hamilton population (COHP) and integrated crystal-orbital Hamilton population (ICOHP) analyses were performed using the LOBSTER program [32–34], taking into account all valence orbitals in the crystal. Similar to the crystal-orbital overlap population (COOP), the COHP analysis provides a quantitative measure of the bond strengths in crystal structures (by –COHP values), where the positive and negative signs represent bonding and antibonding states, respectively.

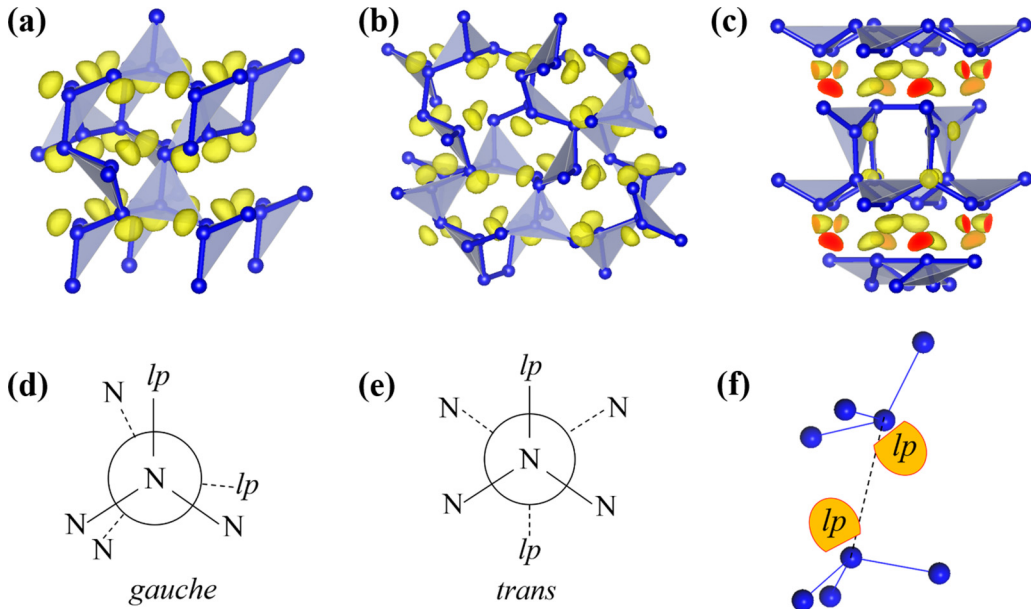


FIG. 2. Calculated electron localization function isosurfaces for (a) the cg structure, (b) the *Pccn* structure, and (c) the *Pba2* structure at 140 GPa. For a clear presentation, a high isovalue of 0.9 is chosen to screen out all σ bonds and show lone pairs only (lobes outside the nitrogen atoms). (d) and (e) Newman projections of *gauche* and *trans* conformers in solid nitrogen. (f) Geometry of interlayer electrostatic interaction in the *Pba2* structure.

III. RESULTS AND DISCUSSION

The cg structure of nitrogen was adopted as the starting structure for the metadynamics simulation since the phase reported by Tomasino *et al.* [4] was synthesized at pressures above the stability field of the cg phase. The metadynamics simulation searches for the low-energy transition pathways leading from the initial energy well (cg) to neighboring minima (new phases) in the potential energy surface, and therefore enables the reconstruction of phase transitions. The present simulation revealed several high-pressure structures of nitrogen, including the previously proposed BP, *C2/c* [35], and *Pba2* [14] structures, at different *P-T* conditions. The most interesting finding, however, is an orthorhombic *Pccn* structure discovered at 2500 K at pressures between 100 and 150 GPa. The transition mechanism between the cg and *Pccn* structures is illustrated in Figs. 1(a) and 1(b). The *Pccn* is a single-bonded structure, in which each atom bonds to three neighbors and carries one lone pair (*lp*) [Fig. 1(b)]. This structure consists of three types of ring structures, N_8 , N_{10} , and N_{12} , fused together in a distorted tetrahedral sp^3 network [Fig. 1(d)]. Similarly, the cg structure is also single-bonded, but it contains only the N_{10} rings [Fig. 1(c)]. The cg \rightarrow *Pccn* transition is depicted in Figs. 1(e) and 1(f); that is, every second vertical array of the N_{10} rings in the cg structure breaks the bonds between the rings and creates new bonds to form a new array of alternating N_8 and N_{12} rings, while the other N_{10} rings keep the integrity but distort notably to accommodate the bonding changes. The resulting structure loses *all gauche helicity* but it is still an energetically favorable configuration.

The geometry of the dihedral angles (of *lp-N-N-lp*) and the resulting *lp-lp* interactions in solid nitrogen were analyzed using the electron localization function [36]. In the cg structure, all dihedral angles have the same *gauche* conformation

[Fig. 2(a) and Fig. 2(d)]. At 140 GPa, the calculated *gauche* angles in the cg structures are $\sim 104.8^\circ$, which are considerably larger than the *gauche* angle in the H_2N-NH_2 molecule ($\sim 91^\circ$) [37]. The *gauche* angles in the cg structure are modified by the bonding groups (N_3 instead of NH_2) and are also enlarged to accommodate the extended sp^3 framework. In the *Pccn* structure [Fig. 2(b) and Fig. 2(e)], 8 out of the total 48 dihedral angles have the *trans* conformation in which the *lp* repulsions are minimized [10,38]. The remaining 40 dihedral angles are all in the *gauche* conformation, of which 20 are between 103.5° and 106.5° , similar to the *gauche* angles in the cg structure, and 16 are at 90.6° , close to the *gauche* angle in H_2N-NH_2 . The right-angle conformer is an energy minimum since it minimizes the two-orbital/four-electron destabilizing interaction between the adjacent lone pairs. The other angles in the *Pccn* structure are 121.1° in nearly ideal staggered conformation. There is no energy maximum *cis* conformation in the *Pccn* structure. This configuration results in a distribution of the single bond lengths in the *Pccn* structure between 1.329 Å and 1.635 Å, as opposed to the unique bond length (1.421 Å) in the cg structure. The *Pba2* structure, on the other hand, has a different structural motif than those of cg and *Pccn* structures. As opposed to the 3D extended sp^3 framework, the *Pba2* structure features a layered geometry with single-bonded nitrogen slabs stacked along the *z* direction [Fig. 2(c) and Fig. 2(f)]. Within the layers, all dihedral angles have the *trans* conformation which provides considerable stability. Between the layers, the gap is filled by lone pairs from the nitrogen atoms on each side of the gap [Fig. 2(c)]. These lone pairs are aligned in a side-on fashion which provides a screening of the nitrogen cores across the gap [Fig. 2(f)]. This geometry reduces the potential energy of the system through electrostatic core-*lp*...*lp*-core interaction.

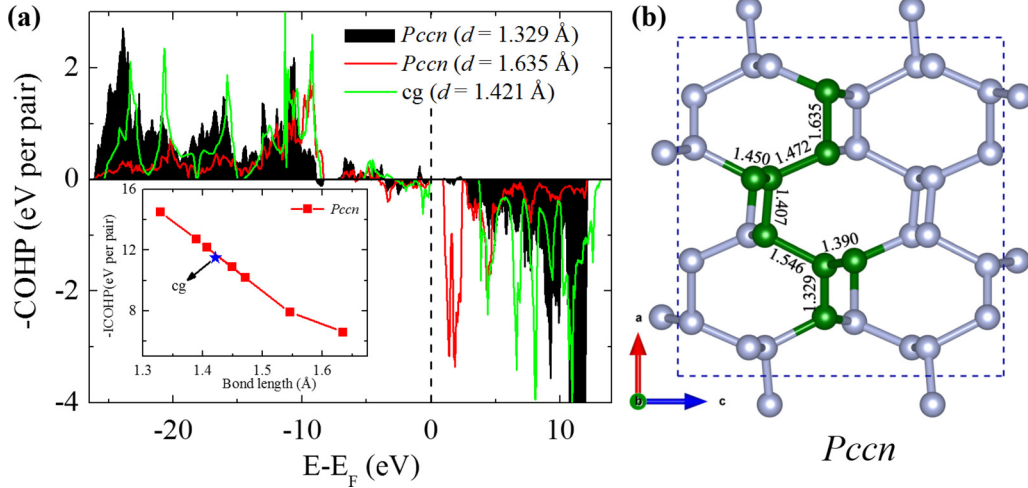


FIG. 3. (a) Calculated $-\text{COHP}$ values for bonded N-N pairs in cg and $Pccn$ structures. The shortest (1.329 \AA) and longest (1.635 \AA) bonds in the $Pccn$ structure were selected for presentation. Inset shows the $-\text{ICOHP}$ values for bonded N-N pairs in cg (1.421 \AA) and $Pccn$ (between 1.329 \AA and 1.635 \AA) structures. (b) Distribution of N-N pairs in the $Pccn$ structure, where atoms are colored in green to guide the eye.

Interaction of this type is expected to be much stronger than the van der Waals interaction which is more favorable at high pressures [39,40].

The strength of the single bonds in the $Pccn$ structure was evaluated using the $-\text{COHP}$ and $-\text{ICOHP}$ analysis, and the obtained results were compared with that of the cg structure [Fig. 3(a)]. Interestingly, a “shorter bond = stronger bond” situation is revealed in the nearly linear relation between the integrated COHP values and the bond lengths, which does not seem to be dependent on the crystal structure (inset). The shortest bond (1.329 \AA) in the $Pccn$ structure has the largest $-\text{ICOHP}$ value (14.52 eV/pair), which sets up a favorable condition for the stability, but the longer bonds go against it and compete. On average, the bond length in the $Pccn$ structure is 1.461 \AA [Fig. 3(b)], slightly greater than that in the cg structure (1.421 \AA). The overall stability of the $Pccn$ structure, therefore, is less than that of the cg structure.

The structural parameters of the $Pccn$ structure (optimized at 137 GPa) are $8e: 0.1638, 0.8230, 0.5504; 8e: 0.6592, 0.6684, 0.5378; 8e: 0.4026, 0.4077, 0.2727; 8e: 0.9074, 0.2019, 0.2573$, with $a = 6.96 \text{ \AA}$, $b = 3.45 \text{ \AA}$, and $c = 6.84 \text{ \AA}$. The experimental XRD pattern reported at the same pressure [4] was used to examine the structures. We found that none of the known theoretical structures alone was able to sufficiently reproduce the experimental XRD pattern, but the combination of the $Pccn$ structure and the $Pba2$ structure predicted by Ma *et al.* [14] (in a 1:2 ratio) appears to be a reasonable match (Fig. 4). This confirms that the synthesized phase is a multiphase mixture. The simulated XRD pattern reveals that the majority of the observed Bragg peaks belongs to the $Pba2$ structure. The two peaks at 10.9° and 11.3° can be uniquely indexed to the $Pba2$ structure, while the two at 9.5° and 12.2° appear to be overlapping with the peaks from the $Pccn$ structure. The two peaks at 8.3° and 14.3° are signature peaks of the $Pccn$ structure, which are indexed to (111) and (121) , respectively. The weak peaks below 8° and those between 19° and 20° can also be uniquely indexed to the $Pccn$ structure. Essentially, most of the 2θ positions of the Bragg peaks in the

experimental XRD can be matched to the theoretical structures. The relative intensities of the peaks however have varying degrees of deviation, in particular for the peak at 20.2° [(213) of the $Pba2$ structure]. This could be due to a slight modification of the structure and the preferred orientation of the crystal. It should also be noted that due to the experimental difficulties, such as weak x-ray scattering of nitrogen and the uncertainties in the background subtraction, the present experiment-theory comparison shows a consistency that supports the presence of the $Pccn$ and $Pba2$ structures but this does not rule out the

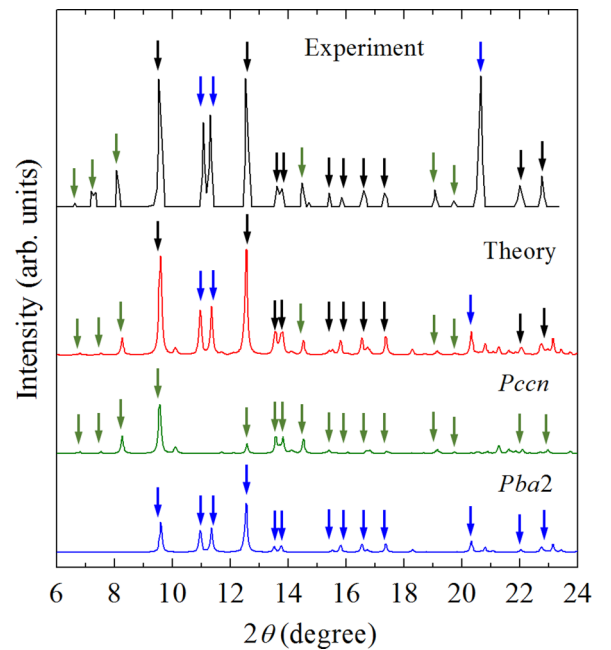


FIG. 4. Calculated XRD patterns for the $Pccn$ structure, the $Pba2$ structure, and the 1:2 mixture of the two structures at 137 GPa , compared with the experimental XRD pattern at the same pressure. The experimental XRD pattern was adapted from Ref. [4].

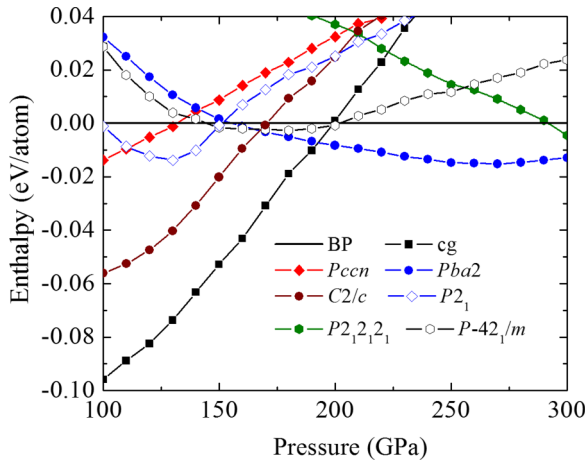


FIG. 5. Enthalpies as functions of pressure for candidate structures of high-pressure nitrogen. The enthalpy of the BP structure is used as the zero-energy reference level.

possibility that other structures, in particular the $C2/c$ [35] and cg [5] structures, may coexist in this P - T region.

The enthalpies of the candidate structures of nitrogen ($H = E + pV$) are compared in Fig. 5 over the pressure range 100–300 GPa. This comparison includes the $Pccn$ structure and several previously predicted structures, namely, cg, BP, $Pba2$, $P2_12_12$, $P-42_1/m$ [14], and $C2/c$. The cg and $Pba2$ structures were found to be the lowest enthalpy structure below and above 190 GPa, respectively, which agrees well with previous calculations [12,14,15]. In the 100–140 GPa range, both the $Pccn$ and $Pba2$ structures have higher enthalpies than the cg structure. This indicates that they are not thermodynamic ground state at 0 K but could be metastable at high temperatures (see later). The experimental observation of the new phase at high temperatures, i.e., above 2500 K, appears to support this conjecture. At 120 GPa, the enthalpy differences between these two structures and the cg structure are about 0.07 and 0.1 eV/atom, respectively, which, in terms of equivalent temperature, are 812 K and 1160 K. In this pressure range the previously predicted $C2/c$ structure [35] is also energetically competitive and therefore could also be a valid candidate. For other structures, since their simulated XRD patterns do not correspond to the experimental observations, they are not considered further.

The mechanical and dynamical stability of the $Pccn$ structure at 140 GPa was established by the phonon calculations [Fig. 6(a)]. The absence of imaginary frequencies in the phonon dispersion relations confirms the stability of the $Pccn$ structure. The $Pccn$ structure is also predicted to be mechanically and dynamically stable at ambient pressure (Fig. 7). This indicates a possibility of quench recovery at ambient conditions in the event of high-pressure synthesis. The maximum optical band reduces its frequencies at ambient pressure but the dispersion profile is retained with an effect of proportionate compression of every band. This can be linked to, and explained by, the volume gain during decompression inducing a reduction in the vibrational frequency of each mode. Notably, the optical branches are nearly flat, revealing nondispersing N-N vibrons in the ring structures. Due to the

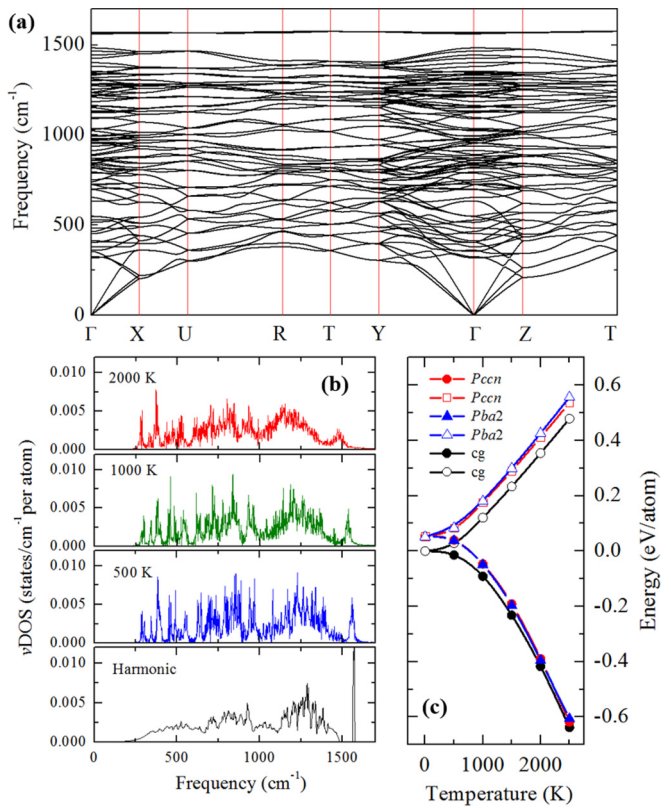


FIG. 6. (a) Phonon dispersion relations for the $Pccn$ structure at 140 GPa. (b) Phonon DOS and temperature-dependent v DOS for the $Pccn$ structure at 140 GPa. (c) The temperature-dependent $H + U_{\text{vib}}$ (open symbols) and $H + F_{\text{vib}}$ (solid symbols) for the $Pccn$, $Pba2$, and cg structures at 140 GPa (see text). The energy of the cg structure at 0 K was used as the zero-energy origin.

particular vibrational modes, one expects that the $Pccn$ and cg structures have different vibrational internal energy U_{vib} and free energy F_{vib} that could compensate for the enthalpy difference. To this end, we estimated the $U_{\text{vib}}[-\partial \ln(Z)/\partial \beta]$ and $F_{\text{vib}}[-\ln(Z)/\beta]$ for the $Pccn$, $Pba2$, and cg structures at 140 GPa using the harmonic approximation [41] in which all vibrational modes are treated as normal modes with the

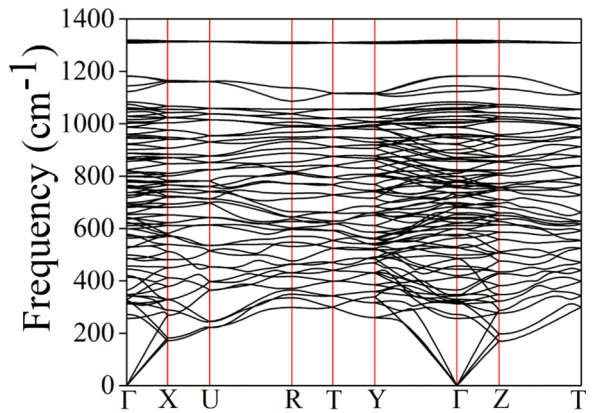


FIG. 7. Phonon dispersion relations for the $Pccn$ structure at 0 GPa.

frequency distribution described by the actual vibrational density of states (v DOS). The v DOS was calculated at five different temperatures between 500 and 2500 K using the single-particle velocity autocorrelation function obtained from the thermal trajectory of a 20 ps *NPT* molecular dynamics simulation, which captures both harmonic and anharmonic vibrations [42]. Figure 6(b) exemplifies the v DOS of the *Pccn* structure at three temperatures, compared with the phonon DOS at 0 K. Clearly, the overall profile of the v DOS is retained at high temperatures even up to 2000 K. Compared with the phonon DOS, the v DOS at finite temperatures have broadened peaks due to greater degrees of freedom, and slightly lowered frequencies due to the unit cell expansion.

The calculated energy sums $H + U_{\text{vib}}$ and $H + F_{\text{vib}}$ for the *Pccn*, *Pba2*, and cg structures at 140 GPa are illustrated in Fig. 6(c) as functions of temperature. Here the enthalpy values (H) are taken from the static calculation (Fig. 5). Taking into account the zero-point contributions, at $T = 0$ K the cg structure is more stable than the *Pccn* and *Pba2* structures by -0.052 and -0.053 eV/atom, respectively [Fig. 6(c)]. When raising the temperature, the internal energies U_{vib} of all structures increase, but the differences of U_{vib} between the structures are nearly constant, signifying the energy equipartition in this temperature regime. The relative stability of the structures is therefore determined by the entropic contributions to the F_{vib} or $-TS_{\text{vib}}$. The F_{vib} are notably lower in the *Pccn* and *Pba2* structures than in the cg structure, suggesting that a phase transition might occur as a consequence of the increased entropies at sufficiently high temperatures (but below the melting point). As shown in Fig. 6(c), the $H + F_{\text{vib}}$ curves bend down, and their differences decrease at high temperatures, suggesting that the *Pccn* and *Pba2* structures become more stable with increasing temperature. With the F_{vib} accounted for, the *Pccn* and *Pba2* structures are only higher in energy than the cg structure by -0.019 and -0.032 eV/atom, respectively, at 2500 K. Given a small energy deficiency, the *Pccn* and *Pba2* structures may therefore be stabilized by kinetics at high temperatures, utilizing the high mechanical stability of the sp^3 covalent networks.

IV. CONCLUSION

In conclusion, we report a single-bonded structure of nitrogen at 2500 K at pressures between 100 and 150 GPa which is likely to be a minor component of the newly synthesized polymeric nitrogen phase in the same *P-T* region. The predicted *Pccn* structure is composed of fused N_8 , N_{10} , and N_{12} rings connected in a way that all lp -N-N- lp dihedral angles are in low-energy *gauche* or *trans* conformations. The simulated XRD pattern of a mixture of the *Pccn* structure and a previously proposed *Pba2* structure matches the experimental data very well. Dynamical stability of the *Pccn* structure is established by phonon calculations which reveal no imaginary frequencies in the entire Brillouin zone. Vibrational free energy calculation utilizing the temperature-dependent v DOS obtained from molecular dynamics simulations shows that the *Pccn* structure is marginally higher in energy than the cg structure (~ 0.02 eV/atom) at 140 GPa and 2500 K, indicating that the structure could be stabilized by kinetics. The present study establishes another single-bonded nitrogen phase after the lab-synthesized cg phase and advances the understanding of the phase diagram of nitrogen under extreme conditions, which will stimulate the study of metastable phases of nitrogen for energy storage applications.

ACKNOWLEDGMENTS

This project was supported by Natural Sciences and Engineering Research Council of Canada (NSERC). H.G. acknowledges financial support from the National Natural Science Foundation of China (NSFC) under Grants No. 51201148 and No. U1530402, the Thousand Youth Talents Plan. Computing resources were provided by the University of Saskatchewan, WestGrid, and Compute Canada. Work at Carnegie was supported by Energy Frontier Research in Extreme Environments Center (EFree), an Energy Frontier Research Center funded by the Department of Energy (DOE), Office of Science, Basic Energy Sciences under Award No. DE-SC-0001057.

-
- [1] F. Cacace, G. de Petris, and A. Troiani, *Science* **295**, 480 (2002).
 - [2] K. O. Christe, W. W. Wilson, J. A. Sheehy, and J. A. Boatz, *Angew. Chem., Int. Ed.* **38**, 2004 (1999).
 - [3] M. Eremets, A. Gavriliuk, I. A. Trojan, D. A. Dzivenko, and R. Boehler, *Nat. Mater.* **3**, 558 (2004).
 - [4] D. Tomasino, M. Kim, J. Smith, and C.-S. Yoo, *Phys. Rev. Lett.* **113**, 205502 (2014).
 - [5] C. Mailhiot, L. H. Yang, and A. K. McMahan, *Phys. Rev. B* **46**, 14419 (1992).
 - [6] B. Hirshberg, R. B. Gerber, and R. I. Krylov, *Nat. Chem.* **6**, 52 (2014).
 - [7] M. J. Greschner, M. Zhang, A. Majumdar, H. Liu, F. Peng, J. S. Tse, and Y. Yao, *J. Phys. Chem. A* **120**, 2920 (2016).
 - [8] W. D. Mattson, D. Sanchez-Portal, S. Chiesa, and R. M. Martin, *Phys. Rev. Lett.* **93**, 125501 (2004).
 - [9] M. M. G. Alemany and J. L. Martins, *Phys. Rev. B* **68**, 024110 (2003).
 - [10] F. Zahariev, J. Hooper, S. Alavi, F. Zhang, and T. K. Woo, *Phys. Rev. B* **75**, 140101 (2007).
 - [11] F. Zahariev, S.V. Dudiy, J. Hooper, F. Zhang, and T. K. Woo, *Phys. Rev. Lett.* **97**, 155503 (2006).
 - [12] X. Wang, Y. Wang, M. Miao, X. Zhong, J. Lv, T. Cui, J. Li, L. Chen, C. J. Pickard, and Y. Ma, *Phys. Rev. Lett.* **109**, 175502 (2012).
 - [13] C. J. Pickard and R. J. Needs, *Phys. Rev. Lett.* **102**, 125702 (2009).
 - [14] Y. Ma, A. R. Oganov, Z. Li, Y. Xie, and J. Kotakoski, *Phys. Rev. Lett.* **102**, 065501 (2009).
 - [15] J. Sun, M. Martinez-Canales, D. D. Klug, C. J. Pickard, and R. J. Needs, *Phys. Rev. Lett.* **111**, 175502 (2013).
 - [16] A. F. Goncharov, E. Gregoryanz, H. K. Mao, Z. Liu, and R. J. Hemley, *Phys. Rev. Lett.* **85**, 1262 (2000).
 - [17] E. Gregoryanz, A. F. Goncharov, R. J. Hemley, and H.-K. Mao, *Phys. Rev. B* **64**, 052103 (2001).

- [18] M. I. Eremets, R. J. Hemley, H. K. Mao, and E. Gregoryanz, *Nature (London)* **411**, 170 (2001).
- [19] M. J. Lipp, J. P. Klepeis, B. J. Baer, H. Cynn, W. J. Evans, V. Iota, and C.-S. Yoo, *Phys. Rev. B* **76**, 014113 (2007).
- [20] E. Gregoryanz, A. F. Goncharov, C. Sanloup, M. Somayazulu, H.-K. Mao, and R. J. Hemley, *J. Chem. Phys.* **126**, 184505 (2007).
- [21] I. A. Trojan, M. I. Eremets, S. A. Medvedev, A. G. Gavriliuk, and V. B. Prakapenka, *Appl. Phys. Lett.* **93**, 091907 (2008).
- [22] R. Martoňák, A. Laio, and M. Parrinello, *Phys. Rev. Lett.* **90**, 075503 (2003).
- [23] R. Martoňák, D. Donadio, A. R. Oganov, and M. Parrinello, *Nat. Mater.* **5**, 623 (2006).
- [24] G. Kresse and D. Joubert, *Phys. Rev. B* **59**, 1758 (1999).
- [25] G. Kresse and J. Hafner, *Phys. Rev. B* **47**, 558 (1993).
- [26] J. P. Perdew, K. Burke, and M. Ernzerhof, *Phys. Rev. Lett.* **77**, 3865 (1996).
- [27] Y. Wang, J. Lv, L. Zhu, and Y. Ma, *Phys. Rev. B: Condens. Matter* **82**, 094116 (2010).
- [28] Y. Wang, J. Lv, L. Zhu, and Y. Ma, *Comput. Phys. Commun.* **183**, 2063 (2012).
- [29] C. J. Pickard and R. J. Needs, *Phys. Rev. Lett.* **97**, 045504 (2006).
- [30] A. Togo and I. Tanaka, *Scr. Mater.* **108**, 1 (2015).
- [31] S. Baroni, S. de Gironcoli, A. Dal Corso, and P. Giannozzi, *Rev. Mod. Phys.* **73**, 515 (2001).
- [32] S. Maintz, V. L. Deringer, A. L. Tchougréeff, and R. Dronskowski, *J. Comput. Chem.* **37**, 1030 (2016).
- [33] R. Dronskowski and P. E. Bloechl, *J. Phys. Chem.* **97**, 8617 (1993).
- [34] V. L. Deringer, A. L. Tchougréeff, and R. Dronskowski, *J. Phys. Chem. A* **115**, 5461 (2011).
- [35] A. R. Oganov and C. W. Glass, *J. Chem. Phys.* **124**, 244704 (2006).
- [36] A. D. Becke and K. E. Edgecombe, *J. Chem. Phys.* **92**, 5397 (1990).
- [37] A. H. Cowley, D. J. Mitchell, M. H. Whangbo, and S. Wolfe, *J. Am. Chem. Soc.* **101**, 5224 (1979).
- [38] Y. Yao, J. S. Tse, and K. Tanaka, *Phys. Rev. B* **77**, 052103 (2008).
- [39] H. Liu, Y. Yao, and D. D. Klug, *Phys. Rev. B* **91**, 014102 (2015).
- [40] X. Dong, A. R. Oganov, A. F. Goncharov, E. Stavrou, S. Lobanov, G. Saleh, G.-R. Qian, Q. Zhu, C. Gatti, V. L. Deringer, R. Dronskowski, X.-F. Zhou, V. B. Prakapenka, Z. Konôpková, I. A. Popov, A. I. Boldyrev, and H.-T. Wang, *Nat. Chem.* **9**, 440 (2017).
- [41] P. Pavone, S. Baroni, and S. de Gironcoli, *Phys. Rev. B* **57**, 10421 (1998).
- [42] Y. Yao, R. Martoňák, S. Patchkovskii, and D. D. Klug, *Phys. Rev. B* **82**, 094107 (2010).